Multi-Span Lateral Slide Laboratory Investigation: Phase II

Final Report
December 2022

BRIDGE ENGINEERING CENTER

IOWA STATE UNIVERSITY

Institute for Transportation

About the Bridge Engineering Center

The mission of the Bridge Engineering Center (BEC) is to conduct research on bridge technologies to help bridge designers/owners design, build, and maintain long-lasting bridges.

About the Institute for Transportation

The mission of the Institute for Transportation (InTrans) at Iowa State University is to save lives and improve economic vitality through discovery, research innovation, outreach, and the implementation of bold ideas.

Technical Report Documentation Page

1. Report No. InTrans Project 22-786	2. Government Accession No.	3. Recipient's Catalog No.
4. Title and Subtitle Multi-Span Lateral Slide Laboratory Investigation: Phase II		**5. Report Date** December 2022
		6. Performing Organization Code

1. Report No. InTrans Project 22-786	2. Government Accession No.	3. Recipient's Catalog No.	
4. Title and Subtitle Multi-Span Lateral Slide Laboratory Investigation: Phase II		**5. Report Date** December 2022	
		6. Performing Organization Code	
7. Author(s) Justin Dahlberg (orcid.org/0000-0002-6184-4122), Zhengyu Liu (orcid.org/0000-0002-7407-0912), Abdalla Alomari (orcid.org/0000-0002-0995-2599, and Brent M. Phares (orcid.org/0000-0001-5894-4774)		**8. Performing Organization Report No.** InTrans Project 22-786	
9. Performing Organization Name and Address Bridge Engineering Center Iowa State University 2711 South Loop Drive, Suite 4700 Ames, IA 50010-8664		**10. Work Unit No. (TRAIS)**	
		11. Contract or Grant No.	
12. Sponsoring Organization Name and Address Iowa Department of Transportation 800 Lincoln Way Ames, IA 50010		**13. Type of Report and Period Covered** Final Report	
		14. Sponsoring Agency Code HR-3037	

15. Supplementary Notes

Visit https://intrans.iastate.edu/ for color pdfs of this and other research reports.

16. Abstract

With slide-in bridge construction (SIBC), the bridge superstructure is constructed off the final alignment and then slid laterally from the temporary worksite onto the in-place substructure. Once the sliding is complete, closure joints between the bridge super- and sub-structure are cast to establish continuity. The cementitious materials and reinforcement design used to complete the closure joints affect when the bridge can be opened to traffic or construction loading.

The goal of this research was to investigate the performance of closure joints using ultra-high performance concrete (UHPC) and noncontact lap-spliced reinforcing steel bar, with a specific focus on determining when a noncontact lap-splice has sufficient strength to either open a bridge or expose it to additional construction loading.

The research was also conducted to explore an alternative material to UHPC—hybrid composite synthetic concrete (HCSC)—which may be able to provide sufficient early-age capacity when used in the same way.

A series of laboratory tests were performed on 96 samples including four noncontact lap-splice connection designs with different rebar development lengths and joint filling materials. A time-dependent pull-out test was performed on each design with a focus on the performance at the material early age. Each sample was loaded with a pull-out force until failure. The ultimate capacity of each sample was captured and analyzed.

Based on the test results, recommendations for the selection of UHPC/HCSC closure joints reinforced with lap-spliced rebars were developed.

17. Key Words accelerated bridge construction—hybrid composite synthetic concrete—lateral slide bridge—noncontact lap-spliced rebar—SIBC—slide-in bridge construction—UHPC—ultra-high performance concrete		18. Distribution Statement No restrictions.	
19. Security Classification (of this report) Unclassified.	**20. Security Classification (of this page)** Unclassified.	**21. No. of Pages** 69	**22. Price** NA

MULTI-SPAN LATERAL SLIDE LABORATORY INVESTIGATION: PHASE II

Final Report
December 2022

Principal Investigator
Justin Dahlberg, Acting Director
Bridge Engineering Center, Iowa State University

Co-Principal Investigators
Brent M. Phares, Research Associate Professor
Zhengyu Liu, Senior Research Scientist
Bridge Engineer Center, Iowa State University

Primary Researcher
Abdalla Alomari, Graduate Research Assistant
Bridge Engineering Center, Iowa State University

Authors
Justin Dahlberg, Zhengyu Liu, Abdalla Alomari, and Brent M. Phares

A report from
Bridge Engineering Center
Institute for Transportation
Iowa State University
2711 South Loop Drive, Suite 4700
Ames, IA 50010-8664
Phone: 515-294-8103 / Fax: 515-294-0467
https://intrans.iastate.edu/

TABLE OF CONTENTS

LIST OF FIGURES

LIST OF TABLES

ACKNOWLEDGMENTS

EXECUTIVE SUMMARY

With slide-in bridge construction (SIBC), the bridge superstructure is constructed off the final alignment and then slid laterally from the temporary worksite onto the in-place substructure. Once the sliding is complete, closure joints between the bridge super- and sub-structure are cast to establish continuity. The cementitious materials and reinforcement design used to complete the closure joints affect when the bridge can be opened to traffic or construction loading.

The goal of this research was to investigate the performance of closure joints using ultra-high performance concrete (UHPC) and noncontact lap-spliced reinforcing steel bar, with a specific focus on determining when a noncontact lap splice has sufficient strength to either open a bridge or expose it to additional construction loading. The research was also conducted to explore an alternative material to UHPC—hybrid composite synthetic concrete (HCSC)—which may be able to provide sufficient early-age capacity when used in the same way.

A series of laboratory tests were performed on 96 samples in four noncontact lap-splice connection designs with different reinforcing steel bar development lengths and joint filling materials. A time-dependent pull-out test was performed on each design with a focus on the performance at the material early age. Each sample was loaded with a pull-out force until failure. The ultimate capacity of each sample was captured and analyzed.

The key findings from this research were as follows:

- The UHPC material strength at an age of 12 hrs was insufficient to fully develop the reinforcement bars. At that time, the pull-out force for all three UHPC lap-splice designs (Design 1, Design 2, and Design 3) was less than 10% of the ultimate capacity at full strength. When the UHPC reached one day in age , Design 1 had a greater capacity than Design 2 or 3, and the rebar stress at failure for Design 1 exceeded the bar yield strength of 60 ksi. At 1.5 days, all UHPC connection designs reached the bar yield strength before failure.

- The compressive strength of HCSC quickly increased to near full strength within the first 12 hrs. In fact, the pull-out force (40 kips) required to fail the HCSC connection (Design 4) exceeded the force at which the reinforcement bar yields (36 kips) at 6 hrs.

- The HCSC samples showed better performance with respect to the ultimate pull-out capacity than the UHPC samples during the earliest stages of material cure (before 1.5 days) when comparing the UHPC samples (Design 1, Design 2, and Design 3) to the HCSC samples (Design 4). HCSC gains strength quicker than the UHPC and could provide a solution for joint fill material if a very accelerated timeline is required (e.g., open bridge to traffic or construction loading in less than 24 hrs).

- The laboratory test results indicated that the confinement condition adjacent to the lap-spliced connections affect the ultimate capacity. As a result, prediction equations with respect

to one- and two-sided restraint situations were established for the estimation of the time-dependent ultimate capacities of each design.

CHAPTER 1. INTRODUCTION

1.1 Background and Problem Statement

Lateral slide-in bridge construction (SIBC) has gained increasing attention as a viable accelerated bridge construction (ABC) approach. With lateral slide construction, the majority of the bridge superstructure is constructed off alignment, typically parallel to the final position, and usually on a system of temporary works. The construction of this portion of the bridge is often completed while the original bridge is still open to traffic. In some instances, portions of the substructure are also constructed while the original bridge is still open to traffic; this is a technique aimed to further reduce traffic impacts.

Once the construction of the superstructure is essentially finished, the original bridge is demolished, and the new substructure construction is completed. Then, and usually over a relatively short period of time (commonly hours to a day), the new bridge superstructure is slid laterally from the temporary worksite onto the in-place substructure. Once the sliding is complete, closure joints between the bridge super- and sub-structure are cast to establish the continuity.

In 2017, the Iowa Department of Transportation (DOT) sponsored a research project titled Lateral Slide of Multi-Span Bridges: Investigation of Connections and Other Details–Phase I to investigate economic and durable design details to use in lateral slide construction with a focus on pier connection details (Liu et al. 2021). The ultimate goals of this research were to develop a bridge that is strong, durable, economical, and constructible using the lateral slide method and to provide recommendations for modifications to the Iowa DOT's bridge design standards.

The research was conducted through multiple tasks: a comprehensive literature review of various details and construction approaches for previously completed lateral slide projects, a survey of state DOTs with related experience to collect information on existing methods and practices, and field monitoring during the slide of a three-span, 300 ft long, steel girder bridge on IA 1 southwest of Iowa City, Iowa.

Field monitoring of the structure corroborated the anecdotal observation of those on site. The design of the bridge and the slide-in methods used worked well. No significant negative response from the substructure was observed during the slide-in, and no cracking was observed on the concrete deck or piers.

Despite the success of the project, one significant question remained. *At what point could the bridge be subjected to construction loads or vehicular loads without compromising the strength and performance of the ultra-high performance concrete (UHPC) closure joint between the bridge pier diaphragm and the pier cap?* The closure pours are the last major step to completing the lateral slide, and identifying how soon the joints achieve the necessary strength could allow for additional time savings.

The high-strength properties of UHPC have led to many successful applications, including using UHPC in connections on bridge structures. Research conducted on UHPC began more than 20 years ago, and the first field application of UHPC in the United States on highway infrastructure was in 2006, and in Iowa. Since then, a significant amount of research has been conducted to explore the application of UHPC in different structural components (Russell and Graybeal 2013).

For example, research has been completed to investigat the longitudinal UHPC closure pour connection in prefabricated deck systems (Yuan and Graybeal 2016). Shafieifar et al. (2018) designed UHPC connections between pier columns and cap beams for seismic and non-seismic regions. Research teams have also used UHPC in the longitudinal connections between adjacent box beams (Yuan and Graybeal 2016, Perry and Seibert 2012, Liu et al. 2022).

In 2014, the Federal Highway Administration (FHWA) published code-like guidance on the design and detailing of noncontact lap-spliced connections filled with UHPC material (Graybeal 2014). In this guidance, when used with UHPC, the lap-splice length, l_s, was specified as at least 0.75 l_d, where l_d is the embedment length. For No. 8 to No. 11 deformed steel reinforcing bars, l_d shall be at least 8 d_b. Clear spacing to the nearest lap-spliced bar should be less than or equal to l_s.

In additional research, Haber et al. (2018) further investigated the effect of the UHPC fiber-volume fraction on UHPC-to-rebar bond strength. The results indicated that the UHPC specimens with fiber-volume fractions less than 2% may not have been able to develop sufficient stress in the embedded bars prior to lap-splice failure, which would cause reduced ductility.

These research projects showed that the UHPC closure joint reinforced with noncontact lap-spliced rebar is a good option for establishing the structural continuity between precast bridge elements, but little research specifically identifying when the connection has achieved sufficient strength had been completed.

1.2 Objective and Approach

The objective of this project was to investigate the performance of the UHPC closure joint reinforced with noncontact lap-spliced rebar with a specific focus on determining when a noncontact lap splice has sufficient strength to either open a bridge or expose it to construction loading. In addition, the research was conducted to explore and compare an alternative material, hybrid composite synthetic concrete (HCSC), that may be able to provide sufficient early-age capacity at less overall cost when used as the closure-joint material.

1.3 Research Plan

Task 1: Summarize Phase I findings and complete literature review
Task 2: Conduct time-dependent noncontact lap-splice strength tests
Task 3: Complete data analysis and develop recommendations

CHAPTER 2. LITERATURE REVIEW

The objective of the literature review was to collect and summarize published information related to the performance of UHPC and HCSC and how they might perform in a closure joint reinforced with noncontact lap-spliced reinforced steel bar.

This work started by reviewing the findings and recommendations presented in the Phase I research (Liu et al. 2021), and the results are summarized in section 2.1.

A comprehensive literature review was conducted for material characteristics and applications of UHPC and HCSC. The results are summarized in sections 2.2 and 2.3, respectively.

The use of contact and noncontact lap-splice connections was reviewed and is presented in section 2.4.

Finally, the key findings from the literature review are summarized in section 2.5.

2.1 Review of the Phase I Work

Phase I work (Liu et al. 2021) aimed to identify and develop economic and durable design details to be used with the lateral slide concept, focusing on pier connection details. The goal of this research (Liu et al. 2021) was to produce a bridge that is strong, durable, economical, and constructible and to provide recommendations for modifications to the Iowa DOT's standards.

To meet this goal, the research team reviewed various construction and design details of previously completed lateral slide-in projects. The team also conducted a survey among state DOTs that may have relevant experience on sliding multi-span bridges to collect information that had never been documented.

Finally, the construction/replacement of a bridge on IA 1 over Old Man's Creek, as shown in Figure 1, was equipped with instrumentation and monitored to gain valuable insights during the lateral slide. The focus was to capture the behavior and effects of the slide on key structural elements.

Superstructure of IA 1 bridge

Substructure of IA 1 bridge with bridge orientation

Figure 1. IA 1 bridge

Table 1 lists the key findings from the literature review and survey, and Table 2 lists the lessons learned from the field monitoring of the IA 1 bridge.

Table 1. Findings from the literature review and survey from Phase I

Parameter	Literature Review and Survey Findings
Number of spans	**2–5 spans:** The whole superstructure was usually built continuously over the piers and slid simultaneously onto the permanent structure **≥6 spans (Max. no. of spans in each slide):** The superstructure was usually divided into units of up to a few spans and then slid into the final position using the SIBC approach
Bridge length and width	- The maximum length using the SIBC method is 2,165 ft - The new bridge will be shorter than the original one not to disturb the traffic on the original bridge - Building a new abutment in front of the original one is a common practice - The new bridge is usually wider than the original bridge due to the increase in traffic volume
Substructure type	- Spread footings and drilled shafts are commonly used - The beam-column frame pier, with a spread footing foundation, is frequently used - It is essential to evaluate the capacity of the substructure and foundation before the slide-in - The substructure should be evaluated for the effect of the uplifting force in the pier column and the overturning of the pier structure, and for the effect of the transverse forces (transverse to the sliding direction), especially for the unguided sliding system, etc.
Challenges	- The limited headroom - The influence on the existing substructure - The large horizontal loading induced by the slide-in process - The stability of the existing bridge and its response during the foundation installation needs to be monitored
Bridge girders	- Both prestressed concrete beam and steel plate girders have been used with SIBC - Both steel and concrete diaphragms were used with the SIBC approach without report of an issue - The lateral forces were applied at all of the diaphragms over the abutment and pier - The diaphragms are expected to be designed as large, rigid members to jack up the bridge
Sliding systems	- Both Teflon pad and roller systems have been used for multi-span bridges - The roller support was commonly used if the bridge length and width were more than 300 ft and 50 ft, respectively - The coefficient of friction is between 7 and 20% for Teflon pads and 5% for roller systems
Superstructure type	- Both steel and concrete temporary structures have been used with the inline setup - The connection and the different settlements between the temporary and permanent structures during the slide-in of the superstructure are critical - Performing trial slides, calculating the settlement and the deflection of the system, and analyzing the moving loads are precautionary measures to cover the concerns related to the slide-in method
Lateral slide forces	The applied force and resistance are not constant throughout the slide-in; thus, the laboratory tests associated with appropriate monitoring are one of the approaches that could be used to measure the difference between them

Table 2. Findings of the monitored bridge from Phase I

Parameter	Results
Acceleration	• Although four accelerometers (A1 through A4) were used during the bridge slide-in, only one (A2) indicated significant bridge acceleration. The A2 accelerometer was installed on the east end of the pier cap, where it was connected to the temporary piers. The maximum acceleration was 0.002 g in the transverse direction.
Tilt	• The maximum tilt caused by the jacking force occurred about the transverse direction and was approximately 0.2 degrees. • The maximum tilt about the longitudinal direction was 0.05 degrees. • All of the gauges measuring the tilt in the transverse direction on Pier 1 showed residual rotation (0.04 degrees) upon completion of the slide. • The pier moment of inertia about the longitudinal direction was greater than that about the transverse direction, and Pier 1 had a larger portion above ground than Pier 2, which resulted in lower lateral stiffness. • When Pier 1 was subjected to the lateral slide impulse forces, the maximum tilt was approximately 0.2 degrees about the transverse direction, which resulted in a maximum displacement of 0.6 in. and a force in the longitudinal direction of 400 kips at the top of Pier 1. • The residual horizontal displacement in the longitudinal direction was calculated utilizing the tilt of 0.04 degrees. This resulted in a displacement of 0.14 in. and a force in the longitudinal direction of about 80 kips.
Displacement	• The results indicated that the permanent pier had less vertical displacement than the temporary structure, which one would expect based on the materials and construction methods associated with each. • The data from the C2 displacement transducer (at the side near the temporary structure) initially showed negative values after the superstructure moved onto the permanent piers, and, as the sliding continued, an uplifting action was observed.
Pile Strain	• The results indicated that an uplifting force of about 95 kips occurred on Pier 1 pile 1. The same behavior was not observed on Pier 2, and both exterior piles (pile 1 and pile 14) on Pier 2 were subjected to downward axial forces. • The calculated results indicated that the moment about the transverse direction (Mx) at the base of Pier 1 ranged from 94 to 101 kip-in. • Comparing this to the moment generated by the forces at the top of the pier cap in the longitudinal direction (80 kips) with a lever arm of 24.5 ft (pier height), those M_X values are quite small. This indicated that the assumption of a fixed boundary at the base of the pier was not accurate and was likely lower in a pile on the pile section. The moment about the longitudinal direction (Mz) of 27 to 86 kips-in was also minimal.
Deck Strain	• For the gauges near Pier 1, the strain data collected from E2 and E10 showed an opposite trend. This indicated that a flexural moment occurred on the deck near Pier 1. Although the data from E8 and E14 (near Pier 2) also indicated a similar flexural bending, the strain magnitude was comparatively small.
Girder Strain	• After a careful investigation of the girder strain data, no conclusions with respect to the superstructure flexural behavior from these girder strain data could be made. A deeper study, such as an analytical analysis/finite element study, could be performed to better interpret these data.

The results from the field monitoring work indicated that flexural bending about the longitudinal direction of the superstructure on the horizontal plane occurred during the slide-in. However, the deck strain data were minimal in magnitude, and the resulting forces were inconsequential to the structure. The superstructure consisting of steel girders and concrete diaphragms also performed well during the slide-in.

Greater strains were measured at the strain gauges installed on the pier piles. Even so, the resulting forces were well below the maximum allowable forces. The residual axial and moment forces were low in comparison to capacity. An uplifting action was captured on one of two bridge piers. An approximate calculation indicated that the greatest forces realized in the longitudinal direction induced by the impulse-pushing load at the top of the pier was about 400 kips, with approximately 80 kips of residual force after the slide. Pier 1 had larger strain responses than Pier 2 in both the longitudinal and transverse directions of the bridge. This could be explained by multiple reasons, such as the different pier height above grade, different friction coefficients, uneven weight distribution, etc.

In general, the sliding process of the multi-span steel girder superstructure over the wall pier went smoothly, and no structural behavior of consequence was observed. Similarly, the results showed that no noteworthy response from the substructure was observed during the slide-in. No visible signs of distress (e.g., cracking) were observed on the piers or at the bridge deck level. Hence, the research team concluded that the superstructure with steel girders and concrete diaphragms provided sufficient strength, stiffness, and resiliency to withstand the temporary- and operational-induced forces accompanying the lateral slide-in method without negative or adverse effects.

Although the Phase I results revealed that the slide-in practice worked well, a question that remained after the completion of construction was regarding the early-age, time-dependent strength of the UHPC closure joint between the superstructure and the pier. This ultimately led to the question of how soon construction or traffic loading should be allowed on the bridge. Consequently, these questions motivated the research team to extend the project into its second phase.

2.2 Ultra-High Performance Concrete (UHPC)

UHPC has gained wide attention in the past decades and has been used in many applications due to its outstanding mechanical properties, including high compressive strength, high ductility (post-cracking tensile ductility), resistance to frost/ice damage, resistance to abrasion, and resistance to alkali-silica. UHPC mix comprises a combination of cement, silica fume, fine quartz sand, high-range water-reducing admixtures, steel fibers, and low water-to-cementitious material (w/cm) ratios ranging from 0.15 to 0.25. Superior mechanical properties can be achieved by adjusting the amount of each component, including coarse aggregate and supplementary materials, to improve a specific property of concrete.

In developing structural design guidance for UHPC and its application in bridge engineering, Graybeal and Hartmann (2003) and Graybeal (2006) conducted extensive material tests,

including compression, tension, shrinkage, etc. The researchers concluded that UHPC material displayed significantly enhanced material properties compared with normal concrete and high-performance-concrete (HPC). Regardless of how it is cured, UHPC exhibits very high compressive strengths with an average 28-day compressive strength as high as 28 ksi. Also, the tensile strength of UHPC is considerably higher than that of normal concrete, both before and after tensile cracking, with an average tensile strength of about 1.3 ksi. As measured from casting through one year, UHPC shows an overall shrinkage of approximately 800 microstrain.

To study the impact of curing conditions and concrete age on the mechanical and durability properties of UHPC, Magureanu et al. (2012) conducted experiments on a 1.6×1.6×6.3 in. (40×40×160 mm) specimen. The researchers applied different curing regimes (i.e., 194ºF [90ºC] and 68ºF [20ºC] with 80 to 90% relative humidity [RH] for 5 days) with a 0.21 water-to-cement (w/c) ratio and different steel fiber (i.e., 0% and 2.5%) constitutions. The researchers found that the specimens attained a compressive strength of about 22 ksi and a modulus of elasticity greater than 7,250 ksi. They also concluded that the flexural characteristics were dependent on the fiber addition and the specimen dimensions. The researchers mentioned that the flexural tensile strength displayed values between 2 and 5 ksi.

Haber et al. (2018) performed an experimental study on six different UHPC materials. The difference between these materials was the constitution of the UHPC materials and the manufacturer/supplier. The researchers evaluated the mechanical properties of these materials based on different test methods (i.e., ASTM International, American Association of State and Highway Transportation Officials [AASHTO], or FHWA Turner-Faribanks Highway Research Center [TFHRC] test methods). The results indicated that initial setting times for the tested mix designs ranged from 4 to 9 hrs, and final setting times ranged from 7 to 24 hrs. Without steam or heat treatments during curing, the UHPCs had compressive strengths above 14 ksi in just 7 days. The compressive strengths for most UHPCs after longer curing periods ranged between 20 and 25 ksi. The Poisson's ratios ranged from 0.14 to 0.17. With respect to the tensile strength, despite varying fiber volume fractions, all of the UHPCs showed similar apparent first cracking strength of about 1.0 ksi. All UHPCs showed load-carrying capacity post-cracking. Regarding the bond strength to precast concrete, all specimens failed by tensile rupture of the precast concrete in the flexural beam bond tests involving UHPCs.

To cover the lack of knowledge in studying the abrasion behavior of UHPC, Zhao et al. (2017) conducted abrasion and nanoscratch tests to investigate the abrasion resistance of UHPC as compared with HPC and to understand the mechanisms that govern the macro behavior. For the abrasion test, the research team used 1 in. thick, 4 in. diameter disks. The disks were soaked in potable water for 24 hrs to ensure a constant moisture state for all specimens. Nanoscratch tests were carried out using a Hysitron Triboindenter nanoindenter with a diamond Berkovich tip. The results indicated that the UHPC abrasion resistance was 50% higher than that of the HPC. In addition, the results indicated that the UHPC paste exhibited a higher scratch resistance than the HPC paste.

Given the foregoing, UHPC became a potential material for connecting the prefabricated bridge elements in structural rehabilitation and ABC. Because of that, many research and field

deployments have been carried out to explore using UHPC as a connection material. For example, in studying UHPC as a choice of overlay for concrete bridge decks, Toledo et al. (2020) conducted early-age and longer-term shrinkage tests and slant-shear tests to evaluate the shear strengths at the bond interface between the UHPC and substructure concrete. The researchers concluded that the early-age shrinkage testing showed approximately 55% of the strain occurred in the plastic state and may not contribute to bond stresses, given the elastic modulus of the UHPC should be small at such early ages. Also, the results showed that the thickest slab experienced greater shrinkage than a thinner slab with the same reinforcement, indicating the reinforcement ratio is more important than the area of steel. In addition, the researchers concluded that the interaction between the UHPC and normal concrete could be successfully achieved without using bonding agents.

Varbel et al. (2020) and Liu et al. (2022) investigated the performance of UHPC as a grouting material to fill the shear keys between adjacent bridge girders. The results indicated that the UHPC-grouted shear keys showed an excellent bond interaction between the UHPC and existing precast bridge girders. As a result, the research teams suggested using UHPC grout for shear keys, and especially UHPCs with compressive strength of more than 16 ksi and 18 ksi at 7 and 28 days, respectively.

2.3 Hybrid Composite Synthetic Concrete (HCSC)

Per the manufacturer, HCSC is a polymer-based basalt fiber-reinforced structural concrete offering optimized mechanical effectiveness, compatibility with adjacent materials, and complete elimination of degradation (Kwik Bond Polymers n.d.). Compared to UHPC, HCSC has more flexible behavior in the linear elastic zone, zero coulombs permeability to moisture and chlorides, and half the setting shrinkage strain. HCSC provides high structural composite behavior in less than 4 hrs at 30–100ºF placement temperatures. HCSC suits existing UHPC dimensional and rebar details but does not require top forming, diamond grinding, post-curing, or temperature conditioning. HCSC could be overlaid with PPC-1121 more rapidly and accommodates differential deflections during placement to develop early rebar engagement strength (Kwik Bond Polymers n.d.). Table 3 lists the material properties of the HCSC.

Table 3. HCSC material properties

Material Property	Standard	Value(s)
Tensile Strength	ASTM C1583, modified	1,700 psi
Flexural Strength	ASTM C78, (third-point, 4×4×12 in.)	2,600 psi
Young's Modulus	ASTM C469	2,500 ksi
High-Temperature Service Characteristics	Maintains > 60% Strength and Stiffening	120°F
Coefficient of Thermal Expansion	ASTM T336	$< 11 \times 10^{-6}$ in/in/°F
Linear Shrinkage	ASTM C157 (initial length @ 4 hours) (initial length @ 24 hours)	400 microstrain 90 microstrain
Abrasion Resistance	ASTM C944 (22 lbs, 2 min)	0.1 grams lost (0.00%)
Permeability	ASTM C1202	0.0 coulombs
Rebar Development Length	NY 701-14E Pullout test for UHPC 7-day cure, conditioned for 24 hrs @ 120°F #6 @ 5 in. and #4 @ 3 in. embedment	6db, rebar yielded
Scaling Resistance	ASTM C672	Not Applicable
Alkali-Silica Reaction	ASTM C1260	Not Applicable

Source: Kwik Bond Polymers n.d.

Table 4 compares the compressive and tensile strengths, modulus of elasticity, and coefficient of thermal expansion for UHPC and HCSC.

Table 4. Comparison of material properties between UHPC and HCSC

Material Property	UHPC	HCSC
Compressive strength	24,000 psi	10,000 psi
Tensile strength	1,200 psi	1,700 psi
Modulus of elasticity	7,000 ksi	2,500 ksi
Coefficient of thermal expansion	$6\text{-}8 \times 10^{-6}$ in/in/°F	$< 11 \times 10^{-6}$ in/in/°F

Sources: Graybeal 2006 and Kwik Bond Polymers n.d.

The comparison indicates that the compressive strength and modulus of elasticity for UHPC are higher than those for HCSC. However, the tensile strength of UHPC is lower than that of HCSC.

Wagner and Krauss (2020) evaluated the bond behavior between deformed reinforcing steel and the HCSC material. The research team cast six 12×9 in. cylindrical specimens, as shown in Figure 2, where three were cast with No. 6 bars embedded 5 in. and the other three were cast with No.4 bars embedded 3 in.

Pull-out test samples during casting   **Pull-out test sample after casting**

Wagner and Krauss 2020, Wiss, Janney, Elstner Associates for Kwik Bond Polymers

Figure 2. Pull-out test sample preparation

All of the specimens were tested in a pull-out test following the test method NY 701-14E (NYSDOT 1997), Anchoring Materials-Chemically Curing, Part B. This test method was specified by the New York State DOT (NYSDOT) Special Specification 557.21010016 to qualify UHPC for use in field-cast joints.

Figure 3 shows a typical pull-out setup following Test Method 701-14E.

Wagner and Krauss 2020, Wiss, Janney, Elstner Associates for Kwik Bond Polymers

Figure 3. Test specimen and setup according to NYSDOT Test Method 701-14E, Part B

11

The results of this test were characterized based on the maximum bar stress achieved, the force-slip displacement relation, and the failure mode (Wagner and Krauss 2020). Bar stress was calculated as the load divided by the nominal area of the No. 4 or No. 6 test bars (0.20 or 0.44 in^2, respectively). All six specimens exhibited bar yield, with rebar pull-out occurring after strain hardening of the rebar. Five of the six specimens exhibited a surface cone in addition to a rebar pull-out. A typical pull-out cone is shown in Figure 4.

Wagner and Krauss 2020, Wiss, Janney, Elstner Associates for Kwik Bond Polymers

Figure 4. Typical pull-out failure

Table 5 shows the results of this test at the age of 7 days.

Table 5. Summary of pull-out test results

Sample ID	Bar Size	Embedment (in.)	Temperature (ºF)	Bar Stress at Yield (psi)	Bar Stress at Ultimate (psi)	Failure Type
A-1	No. 4	3	119.4	Not recorded	88,300	Bar yield and pull-out with cone
A-2	No. 4	3	119.4	68,300	93,200	Bar yield and pull-out with cone
A-3	No. 4	3	121.6	68,400	77,700	Bar yield and pull-out with cone
Average	No. 4	3	120.1	68,300	86,400	–
B-1	No. 6	5	125.1	63,400	74,600	Bar yield and pull-out with cone
B-2	No. 6	5	115.6	63,300	92,100	Bar yield and pull-out with cone
B-3	No. 6	5	119.5	63,900	81,600	Bar yield and pull-out
Average	No. 6	5	120.1	63,400	82,700	–

Source: Wagner and Krauss 2020

At a temperature of 120°F, the embedments of both sets of specimens were sufficient to yield the reinforcing rebars and to develop average bar stress of 86,400 psi (No. 4 bars) or 82,700 psi (No. 6 bars) before failing by bar pull-out. The maximum stress at failure on the No. 4 bars with a 3 in. embedment was slightly greater than that on No. 6 bars with a 5 in. embedment.

2.4 Lap-Spliced Rebar Connections

One of the concepts of ABC is to precast bridge elements and deliver these elements to the field for quick assembly. The advantages of this practice are that it reduces the labor cost and time in the field and that it reduces the uncertainties associated with field conditions. The challenges related to this method are to create a strong joint sufficient to connect the precast elements and to maintain overall structural integrity. One way to create such a joint is to use lap-spliced reinforcement bars grouted with adhesive material, i.e., cement-based material.

Lap-spliced reinforcement connections are either contact or noncontact splices, as shown in **Error! Reference source not found.**.

Figure 5. Lap-splice methods: contact (left) and noncontact (right)

Several studies have been conducted in past decades to investigate the use of different splicing methods, such as lap splices, mechanical splices, and welded splices between structural elements, including columns, beams, joints, walls, and slabs. The results have indicated that various parameters, including lapped length, the ratio of lapped bars, bar diameter, transverse reinforcement, concrete mechanical properties, concrete cover, and concrete casting location, could impact the performance of lap splices (Alyousef et al. 2018, Karabinis 2002, and Najafgholipour et al. 2018).

Schuller et al. (1993), Sanchez and Feldman (2015), and Grant (2015) investigated the force and stress transferred through contact and noncontact lap-splice connections. The results indicated that, in noncontact splices, diagonal compressive struts form between the bars and transfer the forces between the rebars. In a contact, lap-spliced connection, additional lateral stress could be created due to the bar movement. Regarding the lap-splice connection failure patterns, Hassan et al. (2012), Najafgholipour et al. (2018), Mousa (2015), Karabinis (2002), and Tarquini et al. (2019) indicated that the most common failure pattern in the lap-spliced connection is the debonding between the rebar and grout material, which usually occurs at the splice zone due to inadequate lapped length or insufficient confinement reinforcement.

Hamad and Mansour (1996) conducted a study on 17 full-scale slab specimens to check the validity of American Concrete Institute (ACI) provisions about transverse spacing between two reinforcing bars lapped in a noncontact tension splice. Each specimen was reinforced with three lap splices, loaded in flexure, and designed to fail in a splitting mode. The results showed that increasing lap-splice space increased the angle and propagation of cracks. The researchers recommended a limit of 30% of splice length for transverse spacing of noncontact lap splices. They recommended clear spacing of $5d_b$.

Mclean and Smith (1997) conducted experiments to study noncontact lap splices in bridge column-shaft connections. They investigated the effects from several variables, including lap-splice length, lapped bar spacing, and spacing of transverse reinforcement. The researchers concluded that, even with long splice lengths and the full development of noncontact lap splices, confinement reinforcement is still needed.

Mousa (2015) conducted a study to investigate the bond strength and ductility of spliced tension bars in high-strength concrete beams. Mousa conducted a test series of 18 simple beams containing different lap-splice lengths (0, 12, 20, and 27.5 in.) in this investigation. The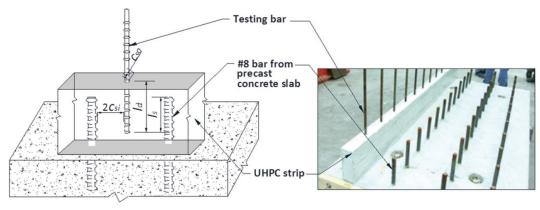 tested beams were 87 in. total length with 8×6 in. cross-sections. The results showed that increasing the bar diameter increased the beam stiffness; thus, both cracking and failure loads increased. Also, the increase in concrete cover on the side and over the reinforcement reduced the number of cracks, stiffness, and ductility of the beam.

Several attempts to grout noncontact lap-spliced connections with UHPC have been documented. For example, studies conducted by Graybeal (2010), Graybeal and Yuan (2014), Fehling et al. (2012), Ronanki et al. (2016), and Harajli (2009) investigated the behavior of the bond between the UHPC and steel reinforcing rebars. The studies found that a high bond strength exists between UHPC and reinforcing steel, making it an effective solution for reducing development lengths.

Graybeal (2010) conducted laboratory experiments to study and evaluate the performance of field-cast UHPC connections linking precast concrete bridge deck components. The tested components simulated a 94.5×84.7 in. portion of a bridge deck that included a 6 in. wide field-cast UHPC connection. A simulated wheel patch was attached near the middle of the simple span to apply load to the specimens. The test setup was developed to simulate the tension–tension lap-splice configuration that may be encountered in a field-deployed closure connection system. According to the test results, the noncontact lap-splice specimens showed higher bond strength than the contact lap-splice specimens.

Graybeal and Yuan (2014) examined the factors that influence bond strength between deformed reinforcement bars and UHPC and developed design guidelines for utilizing field-cast UHPC with innovative connection details. An innovative test specimen and an accompanying loading apparatus were used to conduct direct tension pull-out tests in this study. Precast concrete slabs were used to cast UHPC strips for pull-out testing. The No. 8 bars extended 8 in. (20.3 cm) from the precast concrete slab. UHPC strips were cast on top of the precast slab with the No. 8 bars in the center of the strips. Two No. 8 testing bars were embedded in the UHPC strip, one between each No. 8 bar in the precast concrete slab. The specimen configuration is shown in Figure 6.

Graybeal and Yuan 2014, FHWA

Figure 6. Specimen configuration used by Graybeal and Yuan

The results indicated that, compared to contact lap-splice specimens, noncontact lap-splice specimens exhibit higher bond strength, likely because the fiber reinforcement cannot locally enhance the mechanical resistance of the UHPC in contact lap-splice specimens due to the tight spacing. Also, bond strength increased with increased embedment length (l_d). For bars embedded in the UHPC, the bond strength was nearly linear with the bonded length, indicating improved performance over traditional high-strength concrete.

Haber and Graybeal (2018) investigated the bond strength between UHPC and embedded steel reinforcing bar by conducting direct tension pull-out tests. The research team evaluated five different UHPC-class materials. For the test specimens, the research team used the same test configuration as that used by Graybeal and Yuan (2014). The researchers found that the lap-splice strength increased with a higher fiber content, from 1% to 3%. Based on the test results of Graybeal and Yuan (2014), the FHWA published guidelines for the design and detailing of noncontact lap-splice connections with reinforcing bars embedded in UHPC, as diagrammed in Figure 7.

Connection designs finalizing

Embedment Length of Deformed Steel Reinforcement, ℓ_d

ℓ_d shall be taken as $8d_b$ when:
No. 8 bar and smaller with f_y less than or equal to 75 ksi are used when following conditions are met:
Field-cast UHPC with 2-percent (by volume) steel fiber reinforcement and a compressive strength of at least 14 ksi and Cover $\geq 3d$

ℓ_d shall be taken as $10d_b$ when the previous conditions are met but 75 ksi < fy $\leq$ 100 ksi

ℓ_d shall be increased by $2d_b$ when the fy $\leq$ 100 ksi and with $2d_b \leq$ minimum cover < $3d_b$

Closure Pour Connections Between Prefabricated Bridge Elements regarding the lap-splice length, ℓ_s

For lap splices of straight lengths of deformed steel reinforcement, the lap-splice length, ℓ_s, shall be at least $0.75\ell_d$

Clear spacing to the nearest lap-spliced bar should be less than or equal to ℓ_s. Clear spacing between adjacent bars must also meet the clear spacing requirement defined in Minimum Spacing of Reinforcing Bars.

Interface Shear Connection Between Prefabricated Bridge Deck and Supporting Girder

The design of the connectors attached to the girder shall be completed according to the provisions of AASHTO LRFD Bridge Design Specifications 5.8.4 and 6.10.10

Ducted Substructure Connection Detail

Ducted substructure connections shall be detailed to fully develop the ultimate strength of the embedded deformed steel reinforcing bar. Failure modes to consider include bar pullout from field-cast UHPC, duct pullout from conventional concrete, conventional concrete conical failure around duct, and bar rupture.

The embedment length for No. 8 to No. 11 deformed steel reinforcing bars shall be at least $8d_b$. This length is exclusive of any debonded length.

Minimum Spacing of Reinforcing Bars

Clear spacing between adjacent discrete reinforcements around which UHPC must flow during casting shall be at least 1.5 times the length of the longest fiber reinforcement in the UHPC.

Mechanical Properties of UHPC

Modulus of Elasticity

$E_c = 1550 \sqrt{fc'}$ in ksi

Cracking Tensile Strength

$f_{t,crack} = 0.04\, fc'$

Physical Properties of UHPC

Density

The density of UHPC inclusive of the steel fiber reinforcement may be taken as 155 lb/ft^3

Chloride Ion Diffusion Coefficient

The diffusion coefficient of UHPC may be taken as 2.0×10^{-10} in^2/s

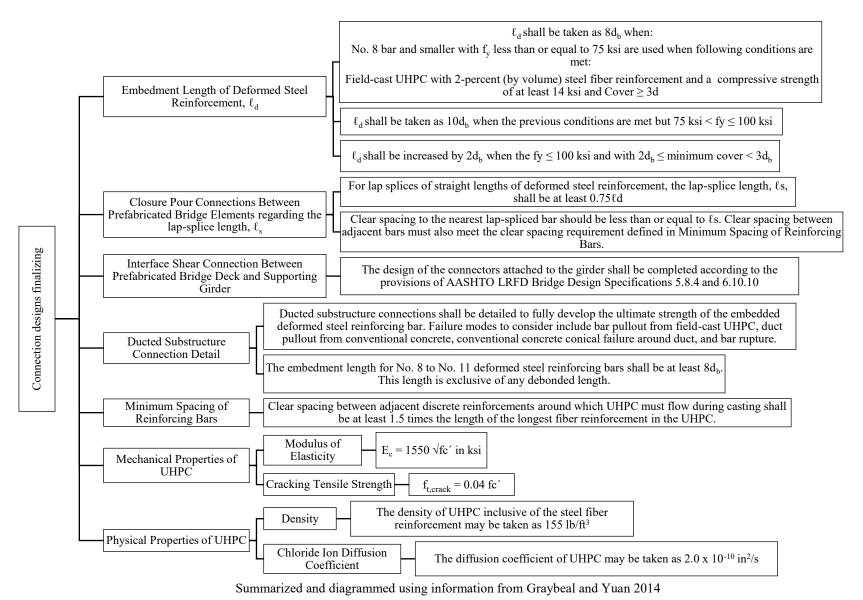Summarized and diagrammed using information from Graybeal and Yuan 2014

Figure 7. Guidance for the structural design of UHPC connection details

In a systematic review of the state-of-the-art developments in reinforced-concrete/UHPC elements, Hung et al. (2021) indicated that, for rebar embedded in UHPC, the tension development length is a fraction of the length needed in conventional concrete. As a result, structural elements can be connected by shorter, straight lengths of rebar in connections that are significantly less complicated than those that use conventional concrete or grout. Reinforcement costs, difficulties in fabrication, and field assembly were all factors that can be improved by specifying field-cast and lap-splice connections with UHPC.

Semendary et al. (2017) studied the early-age behavior of a bridge containing partial-depth shear keys equipped with equally spaced dowel bars and grouted with UHPC. The research team instrumented and monitored a specific bridge built on Sollars Road in Fayette County, Ohio, which was the first adjacent box-beam bridge in the US utilizing reinforced UHPC shear keys. Results showed that, at an early age, even a small change in temperature resulted in greater strains in the portion of the dowel embedded in the shear key. In addition, no cracking of the UHPC shear keys was observed, and thus, the UHPC shear keys performed well.

2.5 Material Cost Comparison

At the time of this report, the material cost comparison of UHPC to HCSC was nearly 2 to 1. It is expected with time and additional popularity of UHPC, costs will comparatively decrease. Each material has its respective performance advantages, but in situations where each meets the minimum performance requirements, the material of lesser cost becomes appealing, especially where widespread use is planned.

2.6 Summary of Literature Review

A comprehensive literature review was conducted to find relevant information on UHPC and HCSC materials and lap-spliced rebar connections. Overall, compared to normal concrete, UHPC offers outstanding material properties, including high compressive strength, tensile strength, and others. Prefabricated bridge elements (PBEs) are commonly used in ABC construction, and UHPC has been used in recent history to provide a reliable lap-spliced connection between PBEs on numerous bridge projects. However, no research studies were identified that specifically investigated the capacities of the lap-spliced UHPC connections at an early age. Understanding the time-dependency of the connection strength is important when the connection is expected to withstand loads at an early age.

Additionally, alternatives for UHPC may exist that provide satisfactory performance as a joint filling material and sufficient early-age capacities. As an example, HCSC, which is designed to achieve its full capacity as early as 4 hrs, is a potential alternative to UHPC.

CHAPTER 3. SPECIMEN DESIGN, CONSTRUCTION, TEST SETUP, AND LOADING PROCEDURES

The main goal of this research was to investigate the performance of the UHPC and HCSC closure joint reinforced with noncontact lap-spliced rebar, with a specific focus on determining when a noncontact lap splice has sufficient strength to either open a bridge or expose it to construction loading. To achieve the goal, direct pull-out tests were designed and carried out.

In this chapter, the specimen design details are discussed in section 3.1. The laboratory construction and loading procedures are presented in sections 3.2 and 3.3, respectively.

3.1 Specimen Design

To investigate the performance of the UHPC and HCSC closure joints reinforced with noncontact lap-spliced rebar, direct tension pull-out tests of four configurations (Design 1, Design 2, Design 3, and Design 4) were completed with one specifically aimed to mimic the closure joint that was used to connect the bridge pier diaphragm and the pier cap of the Hwy 1 Bridge in Iowa. The test specimens were made by casting UHPC or HCSC blocks atop a precast concrete slab, as shown in Figure 8.
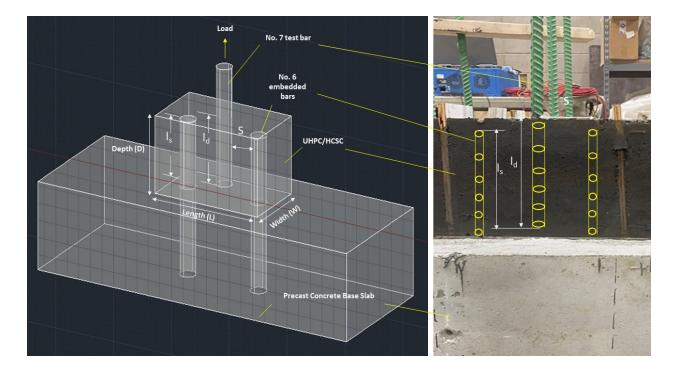

Figure 8 UHPC/HCSC connection configuration

Two protruded rebars (No. 6) extended from the concrete base slab, and one No. 7 rebar was cast into the top layer material for load application.

Table 6 shows the details for each design, and Figure 9 shows the side view of the tested specimens.

Table 6. Specimen design specifications

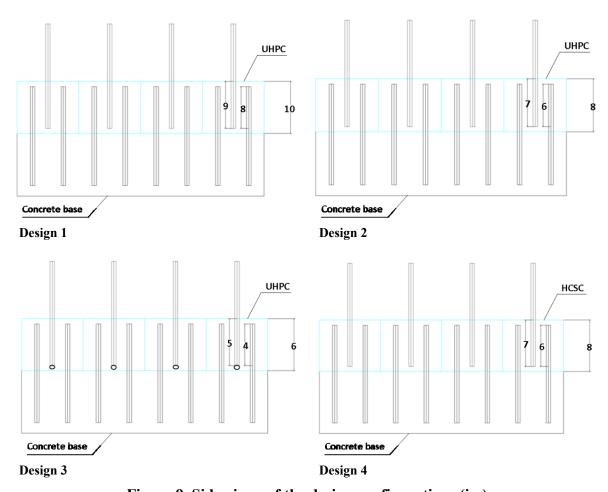| Design ID	Sample geometry (in.)	Design parameters (in.)	Grouting material
Design 1	L = 12 W = 8.25 D = 10	$l_d = 9$ $l_s = 8$ S = 4	UHPC
Design 2	L = 12 W = 8.25 D = 9	$l_d = 8$ $l_s = 7$ S = 4	UHPC
Design 3	L = 12 W = 8.25 D = 6	$l_d = 5$ $l_s = 4$ S = 4	UHPC
Design 4	L = 12 W = 8.25 D = 9	$l_d = 8$ $l_s = 7$ S = 4	HCSC

Figure 9. Side views of the design configurations (in.)

Each specimen was designed with a length (L) of 12 in. and a width of 8.25 in. The height of each sample changed with the reinforcement designs. Design 1 was designed identical to the connection (pier diaphragm) used on the steel girder bridge on IA 1 southwest of Iowa City (Liu et al. 2021), with the development length, l_d, equal to 9 in. and rebar overlap length, l_s, equal to 8 in. Figure 10 shows the pier details of the IA 1 bridge.

Plan view of pier diaphragm
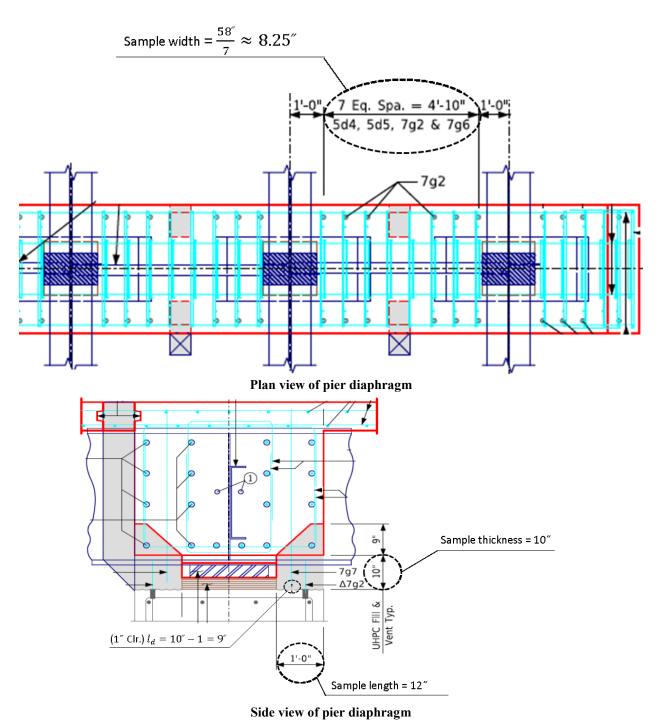
Side view of pier diaphragm

Figure 10. Details of pier diaphragm on IA 1 bridge

Designs 2 and 3 were designed following the FHWA published guidance (Graybeal 2014) regarding the design configuration. Design 2 was designed with a shorter development length of l_d of 8 in. and an l_s of 7 in. Instead of utilizing deformed rebar as used in Designs 1 and 2, Design 3 utilized round-headed bar embedded into the top layer material (UHPC), which reduced l_d to 5 in. and l_s to 4 in. Design 4 was identical to Design 1, except the grouting material was changed to HCSC.

UHPC was used in the first three designs (Design 1, Design 2, and Design 3). The UHPC material used in this project was CT25, which is produced and provided by COR-Tuf UHPC. This was the same material used in the joint construction of the Hwy 1 bridge over Old Man's Creek southwest of Iowa City for the Phase I project. A total of 34 ft^3 (1.3 yd^3) of UHPC was prepared in seven batches. Table 7 shows the UHPC mix proportions used in the project.

Table 7. UHPC mix design

Material	Amount (lb/yd^3)
Cement	1,311.4
COR-Tuf UHPC	1,081
Fine Aggregate	1,428.1
Steel Fiber	265.4
Premia 150	64.5
Optima 100	46.6
CI 100	47.8

The UHPC mix consisted of portland cement, Cor-Tuf UHPC material, fine aggregate, Premia 150 (high-range water reducing admixture), Optima 100 (plasticizer water reducer), CI 100 (corrosion inhibitor), and high strength, high carbon steel fibers (see https://cor-tuf.com/product-information/#). The steel fiber used in the UHPC mix had a diameter of 0.008 in. with a length of 0.5 in. The steel tensile strength was specified to be 413 ksi, with a Young's modulus of 30,458 ksi and a density of 0.28 lb/in^3.

In Design 4, the research team replaced the UHPC with HCSC to investigate whether it could be used as an alternative to UHPC. The HCSC mix proportions used in the project are shown in Table 8.

Table 8. HCSC mix design proportions

HCSC Mix Components	Amount (lb/yd^3)
MEKP	6
HCSC Blended Aggregates	3,000
HCSC Binder Resin	333.6

A total of 11 ft^3 (0.41 yd^3) of the HCSC mixture was prepared, consisting of a hybrid co-polymer resin binder, graded aggregates, and an MEKP catalyst, which was a clear, colorless solution of methyl ethyl ketone peroxide in a mixture of dimethyl phthalate and an ester plasticizer.

The steel reinforcement used for this project included No. 5 uncoated rebar with a diameter of 0.625 in. for the precast concrete slab reinforcement, epoxy-coated No. 6 rebar with a diameter of 0.75 in. for the reinforcement protruding from the base slab, and No. 7 epoxy-coated deformed rebar for Designs 1, 2, and 4 and headed bars with a diameter of 0.875 in. for the Design 3 noncontact lap-spliced reinforcement, as shown in Figure 11. The bearing area of the head was 5 A_b, or 3 in^2.

No.6 Epoxy-coated deformed rebars	No.7 Epoxy-coated headed rebars

Figure 11. Epoxy-coated rebar

3.2 Specimen Construction

To build and cast the precast concrete base slabs, formwork for eight 4×4×1 ft specimens was constructed. Double-layers (top and bottom) of No. 5 reinforcement spaced at 12 in. on center were tied and placed into each form, followed by the protruding No. 6 rebars tied vertically into each slab. The process is shown in Figure 12.

Vertically-fixed embedded rebars

Concrete placement

Filling the concrete slabs

Concrete slabs after concrete placement

Finishing the surface of the concrete slabs

Readied concrete slabs with embedded rebars

Figure 12. Preparing the concrete base slabs

Immediately after concrete placement, the concrete top surface was finished using a hand brush to form a roughened surface to aid the bond between the base slab concrete and the UHPC/HCSC strips, as shown in Figure 12 (bottom left). Seven days after casting the concrete slabs, the formwork was removed. The readied concrete slabs are shown in Figure 12 (bottom right).The next step was to assemble the formwork for the UHPC and HCSC strips. As shown in Table 6, each strip consisted of four 12×8.25 in. (length × width) discontinuous specimens. The details of this step are shown in Figure 13.
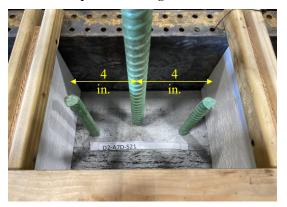
Building the formwork to cast the filling

Vertical setup of the testing bars

Installing 0.5 in. divider to form discontinuous samples

Dimensions for testing deformed bar

Figure 13. Preparing UHPC/HCSC specimen strips

After that, UHPC/HCSC materials were placed to complete the noncontact lap-splice joint of each specimen. In total, 34 ft^3 of UHPC was mixed with 5 ft^3 in each batch. Figure 14 shows the mixing and casting process for the UHPC.

Preparing UHPC batches quantities

Mixing UHPC constituents using 5 ft^3 mixer

Pouring the UHPC in the forms

Specimen after pouring UHPC

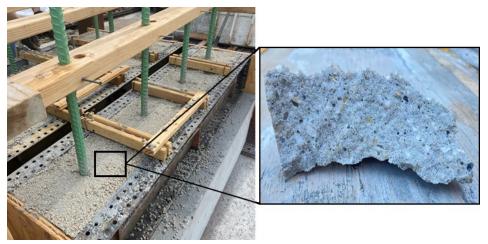**Figure 14. Casting procedure for UHPC specimens**

The UHPC strips were cast at room temperature.

HCSC was mixed outside the structural lab at a temperature of about 80°F. In total, 11 ft^3 of HCSC was mixed with a maximum of 2 ft^3 in each batch. Figure 15 shows the placement of the HCSC.

Preparing the constituents and equipment

Mixing the non-flowable HCSC

Cast HCSC samples and HCSC texture

Figure 15. HCSC mixing process and sample completion

The completed specimens for the UHPC and HCSC strips, located on top of a concrete base slab, are shown in Figure 16.

UHPC sample strips   **HCSC sample strips**

Figure 16. Completed UHPC and HCSC strips

3.3 Test Setup and Loading Procedures

Figure 17 shows the test apparatus and specimen locations.

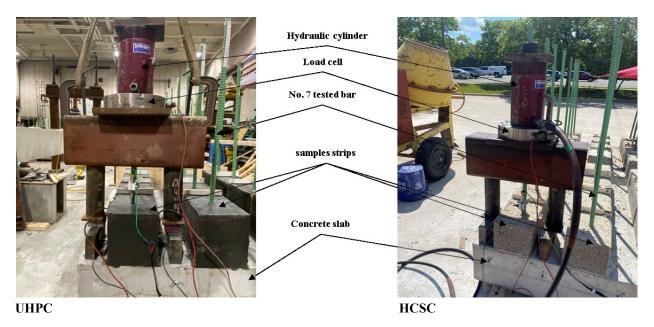**UHPC**   **HCSC**

Figure 17. Experimental test setup

The hydraulic cylinder and load cell were placed on the steel frame, and the steel frame was placed on top of the concrete slab. The concept of the test is that, when the tension (pull-out) force is applied to the testing bars, the load system reacts against the slab through the steel frame. Thus, the load is transferred from the testing rebar to the base concrete through the surrounding materials (UHPC or HCSC) and the embedded rebars. A load cell located between the top of the steel frame and the hydraulic cylinder measured the load applied to the tested rebar.

During the test, displacement and strain gauges were installed to measure the specimen responses when subjected to the pull-out force. Figure 18 shows a typical instrumentation setup on the Design 2 specimen.

Figure 18. Testing instrumentation

One displacement sensor was attached to the testing bar to measure relative displacement between the bar and the UHPC or HCSC sample surface. Each sample had a strain gauge and a deflection transducer installed on opposing sides of it to help quantify any observational evidence of force transfer to the edge of the specimen and relative displacement between the specimen and the base slab, respectively. The collection of strain and relative displacement data was secondary to the primary goal of time-dependent pull-out strength. Accordingly, the results of displacement and strain data are not included in this report.

A timeline of tests was developed to measure the time-dependent bond strength of both the UHPC and HCSC samples. Figure 19 shows the time after initial material placement when the UHPC and HCSC samples were tested.
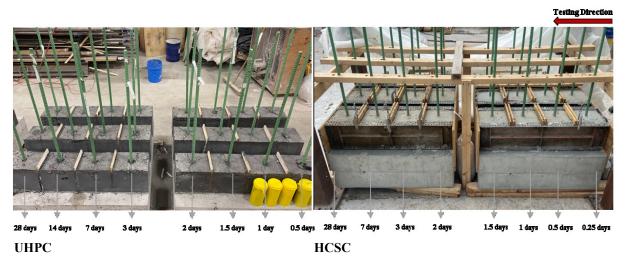
Testing Direction

28 days 14 days 7 days 3 days 2 days 1.5 days 1 day 0.5 days 28 days 7 days 3 days 2 days 1.5 days 1 days 0.5 days 0.25 days

UHPC   HCSC

Figure 19. Final specimen testing timelines for UHPC and HCSC samples

The initial plan was to begin testing the UHPC samples 6 hrs after placement. Upon removal of the forms, the team observed that the UHPC was still soft to the touch, as shown in Figure 20 (left).

Unhardened UHPC at 6 hrs   **Hardened HCSC at 6 hrs**

Figure 20. UHPC and HCSC materials at 6 hrs.

Accordingly, the test of UHPC samples started at 12 hrs when the samples gained sufficient hardness. Subsequent tests occurred at 24 hrs, 36 hrs, 48 hrs, 72 hrs, 7 days, 14 days, and 28 days.

The HCSC samples hardened in a shorter time period, so the research team had the opportunity to start testing this connection at the age of 6 hrs, as shown in Figure 20 (right). The HCSC samples were then tested at 12 hrs, 24 hrs, 36 hrs, 48 hrs, 72 hrs, 7 days, and 28 days.

CHAPTER 4. MATERIAL PROPERTY TEST RESULTS

Compression tests were conducted to evaluate the material properties of the UHPC and HCSC at times corresponding to the connection tests. The results are presented in this chapter.

Alongside each group of pull-out test samples, a set of three test cylinders were prepared for the testing of the compressive strength at each time point. Each cylinder was 3 in. in diameter and 6 in. in height, as shown in Figure 21.

3 in. diameter × 6 in. UHPC cylinders   3 in. diameter × 6 in. HCSC cylinders

Figure 21. Compression test cylinders

The compressive strength tests for both UHPC and HCSC were conducted following ASTM C39/C39M-21.

4.1 UHPC

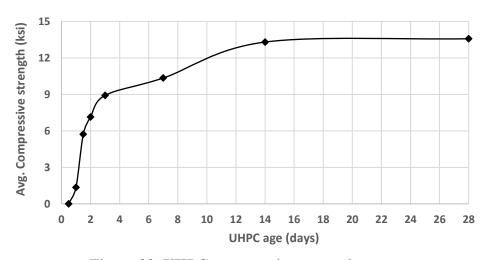Figure 22 shows the average compressive strength results for the UHPC cylinders.

Figure 22. UHPC compressive strength vs. age

The results indicated that the UHPC had an average compressive strength of 1.4 ksi at 24 hrs and 5.7 ksi at 36 hours. The average compressive strength was about 7 ksi and 9 ksi at 48 hrs and 72 hrs, respectively. At 7 days, the average compressive strength was 10.4 ksi, and it increased to about 13.3 ksi at 14 days and 13.6 ksi at 28 days. Note that, 12 hours after casting the UHPC, the specimens did not gain enough strength to complete the compression tests.

As a means of comparison to previously developed compressive strength prediction, the research team used equation (1), created by Graybeal (2006), to calculate the early-age time-dependent compressive strength of UHPC.

$$f'_{c,t} = f'_c \left[1 - e^{-\left(\frac{t-0.9}{3}\right)^{0.6}}\right] \tag{1}$$

where, t is any time after 0.9 days after casting, f'_c is the 28-day compressive strength, and $f'_{c,t}$ is the calculated compressive strength at a specific time. Figure 23 compares the time-dependent compressive strength measured during the test and predicted results utilizing equation (1).
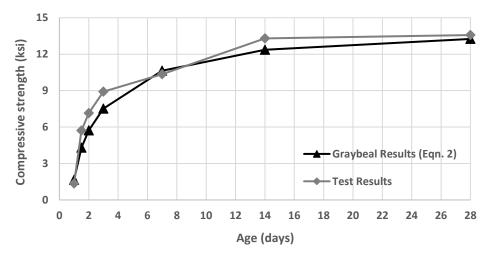

Figure 23. Comparison of compressive strength test results with the predictions by equation (1)

The results showed that the compressive strength measured in the test compared well with the outcomes of the equation developed by Graybeal (2006).

4.2 HCSC

Figure 24 shows the average compressive strength results for the HCSC used in this project.
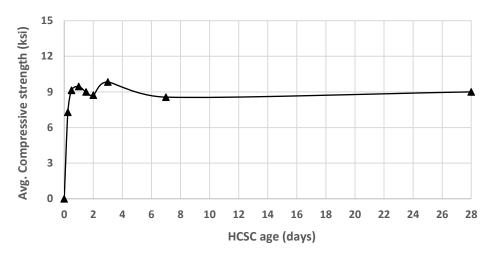
Figure 24. HCSC average compressive strength vs. age

The results show that the average compressive strength of HCSC increased to 9.1 ksi during the first 12 hrs, after which, the compressive strength remained relatively constant. The compressive strength was about 9 ksi at 7 days. This result was consistent with the manufacturer data sheet (Kwik Bond Polymers n.d.), which stated that the compressive strength at 7 days is about 10 ksi.

CHAPTER 5. PULL-OUT TEST RESULTS

This chapter presents the results of the Design 1, 2, 3, and 4 pull-out tests in sections 5.1 through 5.4, respectively, and discusses the results in section 5.5. Designs 1 though 3 used UHPC and Design 4 used HCSC.

5.1 Design 1

As previously mentioned, three UHPC samples were tested for Design 1 at each prescribed early age. Table 9 shows the ultimate capacities for the Design 1 samples and the average capacities at each test point in time.

Table 9. Ultimate capacities of Design 1 samples (kips)

Age	Sample 1	Sample 2	Sample 3	Average
0.5 day (12 hrs)	2.2	3.1	3.2	2.8
1 day (24 hrs)	38.9	43.0	46.2	42.7
1.5 days (36 hrs)	45.0	54.5	54.6	51.4
2 days (48 hrs)	43.5	39.4	43.7	42.2
3 days (72 hrs)	53.7	48.3	46.9	49.6
7 days	57.6	57.2	64.5	59.8
14 days	61.8	59.0	66.9	62.5
28 days	48.8	53.2	60.8	54.2

Design 1 used an embedment length of 10 d_b and splice length 0.8 l_d.

Figure 25 shows the ultimate pull-out capacity ranges for the Design 1 specimens with the minimum, maximum, and average capacities.
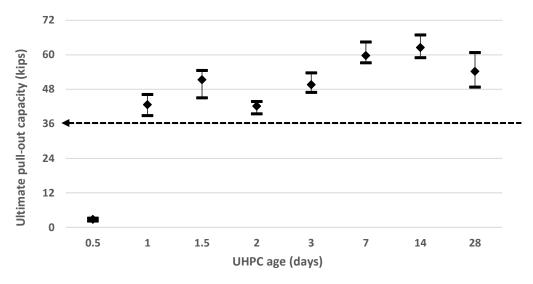
Figure 25. Capacity results vs. age for Design 1

The black dashed line represents the rebar yield capacity of 36 kips at the allowable yield strength of 60 ksi. The results also indicated that, after the UHPC connections achieved an age of 24 hrs (1 day), the failure occurred at a load greater than the load at which the rebar yields. See section 5.5 for possible reasons for the slight decrease in capacity at ages 2 and 3 days.

The average ultimate capacity for the specimens tested at 0.5 days after casting was as low as 2.8 kips with a significant increase to 42.7 kips at 1 day. At 1.5 days, the results showed a further increase in the average value to approximately 51 kips. After that, no significant increase in the ultimate strength occurred. The results also showed that, after the UHPC joint material achieved an age of 24 hours, the failure occurred after the rebar achieved the yield point.

During the entire test, seven failure modes were identified: transverse splitting, longitudinal splitting, diagonal splitting, conical surface failure, all direction splitting, pull-out failure, and debonding at the interface between the testing sample and the concrete base. Examples of all observed failure modes are shown in Figure 26.
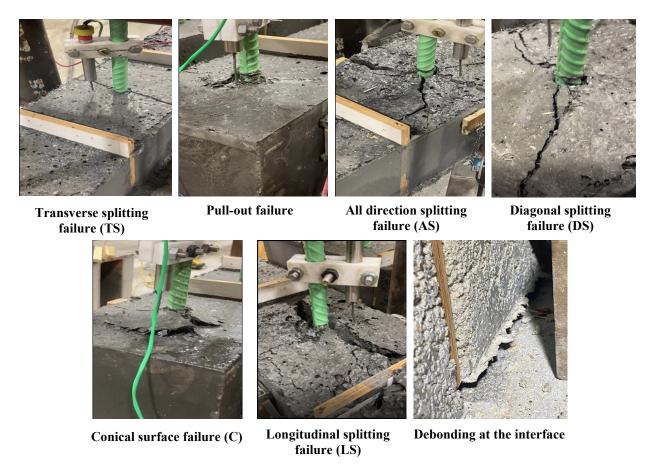
Transverse splitting failure (TS)

Pull-out failure

All direction splitting failure (AS)

Diagonal splitting failure (DS)

Conical surface failure (C)

Longitudinal splitting failure (LS)

Debonding at the interface

Figure 26. Examples of observed failure modes

Design 1 specimens experienced six of the seven failure modes, transverse splitting, diagonal splitting, conical surface failure, all direction splitting, pull-out failure, and debonding at the interface, as shown in Figure 27.

Testing direction

| 0.5 | 1 | 1.5 | 2 | 3 | 7 | 14 | 28 |

Age (days)

AS=all direction splitting, C=conical surface, DS=diagonal splitting, TS=transverse splitting

Figure 27. Failure modes in Design 1

The most common failure was transverse splitting, which initiated around the testing bar and propagated to the specimen sides. Other failure modes were uncommon, as few specimens experienced them. The diagonal splitting failure initiated near the testing bar and propagated toward the sides diagonally. A conical surface failure occurred around the testing bar. In one sample, debonding occurred at the interface between the UHPC and base concrete slab.

5.2 Design 2

For Design 2, three UHPC samples were tested at each prescribed early age. An embedment length of $8d_b$ and splice length of $0.8l_d$ was used. The side cover of $2d_b$ and rebar spacing of $4.5d_b$ was constant through all tested specimens. Table 10 shows the test results for the second design at each test time point.

Table 10. Ultimate capacities of Design 2 samples (kips)

Age	Sample 1	Sample 2	Sample 3	Average
0.5 day (12 hrs)	1.3	0.7	1.6	1.2
1 day (24 hrs)	21.6	21.1	20.8	21.2
1.5 days (36 hrs)	41.1	32.9	35.9	36.6
2 days (48 hrs)	34.9	30.9	32.3	32.7
3 days (72 hrs)	31.3	28.9	39.6	33.3
7 days	48.8	55.6	47.3	42.2
14 days	57.9	48.3	52.9	53.0
28 days	46.1	45.0	46.0	45.7

Figure 28 shows the capacity ranges for the Design 2 specimens with the minimum, maximum, and average capacities.
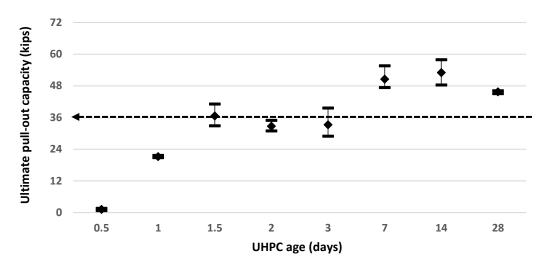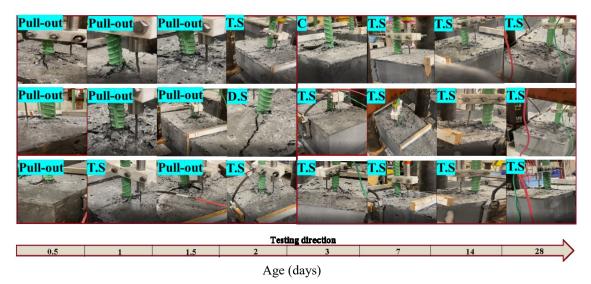

Figure 28. Capacity results vs. age for Design 2

The black dashed line represents the rebar yield capacity of 36 kips at the allowable yield strength of 60 ksi. The results showed that, after the UHPC joint achieved 1.5 days of age, the failures occurred at a load at approximately the yield point of the rebar or higher.

Similar to the results for Design 1, the capacities at 12 hrs for the Design 2 samples were minimal. From 12 to 24 hrs, the average capacities increased dramatically to 36.6 kips. After that, no significant increase in the ultimate strength occurred.

Figure 29 shows the failure modes for all of the Design 2 specimens.

Testing direction

| 0.5 | 1 | 1.5 | 2 | 3 | 7 | 14 | 28 |

Age (days)

C=conical surface, DS=diagonal splitting, TS=transverse splitting

Figure 29. Failure modes in Design 2

The two common failure modes for Design 2 specimens were pull-out failure and transverse splitting. Conical surface and diagonal splitting failures were not common. Given the embedment length for Design 2 was reduced compared to Design 1, more pull-out failures occurred at the early age of the material.

5.3 Design 3

Similar to Designs 1 and 2, three UHPC samples were tested each time for Design 3. An embedment length of $6d_b$ and splice length of $0.8l_d$ were used for the Design 3 samples. The side cover of $2d_b$ and bar spacing of $4.5d_b$ were constant throughout all tested samples. Table 11 shows the test results for the Design 3 specimens.

Table 11. Ultimate capacities of Design 3 samples (kips)

Age	Sample 1	Sample 2	Sample 3	Average
0.5 day (12 hrs)	2.4	1.4	0.7	1.5
1 day (24 hrs)	24.5	21.2	8.1	17.9
1.5 days (36 hrs)	20.9	43.6	41.3	35.3
2 days (48 hrs)	26.2	19.8	29.7	25.2
3 days (72 hrs)	35.5	32.0	56.5	41.4
7 days	41.5	48.3	42.4	44.1
14 days	50.1	62.0	50.0	54.0
28 days	34.7	39.5	38.9	37.7

Figure 30 shows the capacity ranges for the Design 3 specimens with the minimum, maximum, and average capacities.
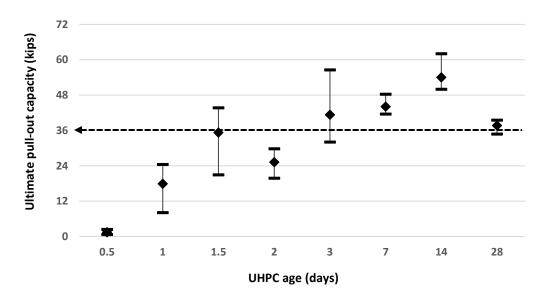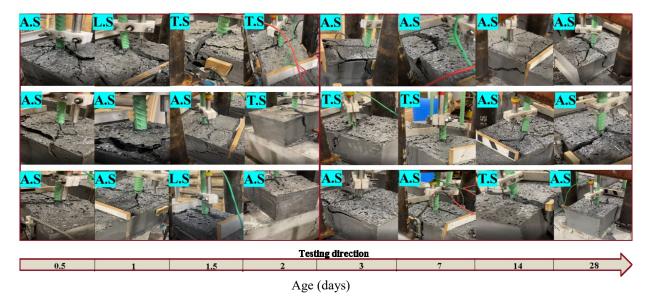

Figure 30. Capacity results vs. age for Design 3

The black dashed line represents the rebar yield capacity of 36 kips at the allowable yield strength of 60 ksi. The results showed that the first time a specimen reached the rebar yield point was when the UHPC reached 1.5 days.

Similar to the results in Designs 1 and 2, the capacities at 12 hrs for the Design 3 samples were minimal. From 12 to 24 hrs, the average capacities increased dramatically to 36 kips. After that, the capacities increased slightly.

Figure 31 shows the failure modes for all Design 3 samples.

Testing direction

| 0.5 | 1 | 1.5 | 2 | 3 | 7 | 14 | 28 |

Age (days)

AS=all direction splitting, LS=longitudinal splitting, TS=transverse splitting

Figure 31. Failure modes in Design 3

All direction splitting was the most common failure type for the Design 3 specimens. While applying a tension force on the testing rebar, the bearing face of the rounded-head rebar embedded deep within the specimen pushed against the surrounding UHPC resulting in cracks originating at the rebar head and propogating in all directions. Transverse splitting and longitudinal splitting were also observed in a few samples.

5.4 Design 4

Three HCSC specimens were tested for Design 4 at each prescribed early age. An embedment length of $10d_b$ and splice length of $0.8l_d$ were used. The side cover of $2d_b$ and bar spacing of $4.5d_b$ were constant throughout all tested samples. Table 12 shows the ultimate capacity test results for the Design 4 samples at all testing ages with their average values.

Table 12. Ultimate capacities of Design 4 samples (kips)

Age	Sample 1	Sample 2	Sample 3	Average
0.25 day (6 hrs)	39.6	40.2	40.5	40.1
0.5 day (12 hrs)	44.3	40.6	42.4	42.5
1 day (24 hrs)	50.8	47.4	52.8	50.3
1.5 days (36 hrs)	47.9	39.2	49.7	45.6
2 days (48 hrs)	56.0	55.4	51.1	54.1
3 days (72 hrs)	53.0	59.5	58.3	56.9
7 days	64.5	56.3	60.6	60.4
28 days	57.1	61.3	58.0	58.8

42

Figure 32 shows the capacity ranges for the tested specimens in Design 4 with the minimum, maximum, and average capacities.
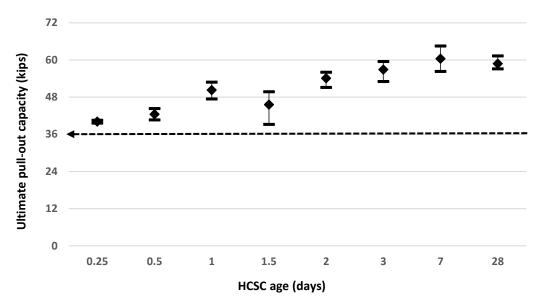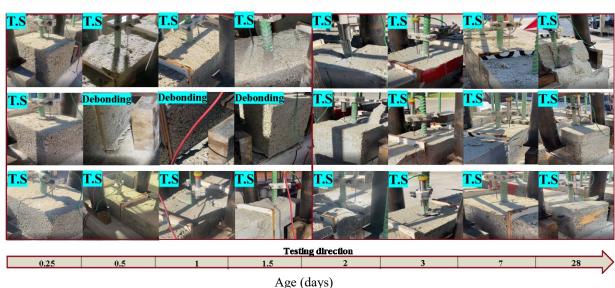

Figure 32. Capacity results vs. age for Design 4

The black dashed line represents the rebar yield capacity of 36 kips at the allowable yield strength of 60 ksi. The results show the Design 4 specimens achieved an average pull-out capacity of approximately 40 kips, which is greater than the force required to yield the rebar, when the material was 6 hrs old. The HCSC specimen strength increased rapidly within the first 6 hours and progressively gained strength at a slower pace over the next 28 days when the average capacity was determined to be approximately 60 kips.

Figure 33 shows all failure modes related to each Design 4 sample.

Testing direction

| 0.25 | 0.5 | 1 | 1.5 | 2 | 3 | 7 | 28 |

Age (days)

TS=transverse splitting

Figure 33. Failure modes in Design 4

Transverse splitting was the most common failure type for the Design 4 samples. Debonding at the interface between the HCSC sample and concrete slab, although it occurred on three samples, was not considered a common failure type.

5.5 Result Discussion

To understand the development of the strengths of the HCSC and UHPC, the time-dependent compressive strength data obtained during the material tests were normalized with respect to the strength at 7 days after casting. The normalized compressive strengths for the UHPC and HCSC were calculated by dividing the compressive strength data by the corresponding 7-day value (10.34 ksi for UHPC and 8.56 ksi for HCSC). Figure 34 shows the normalized compressive strength as a function of time for both materials.
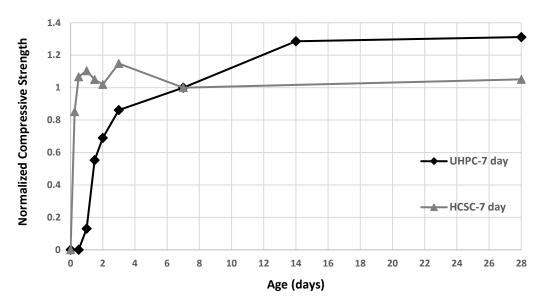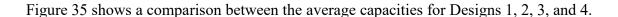
Figure 34. Normalized compressive strength of UHPC and HCSC as a function of time

As shown in Figure 34, the UHPC at 1 day after casting had about 13% of its 7-day value. At an age of 1.5 days, the UHPC achieved 55% of its 7-day value. At the age of 3 days, the UHPC achieved 86% of its 7-day value. On the other hand, as early as 6 hours after casting, the HCSC achieved approximately 85% of its 7-day value.
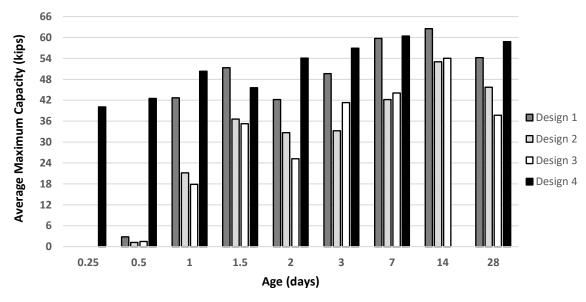
Figure 35 shows a comparison between the average capacities for Designs 1, 2, 3, and 4.

Figure 35. Average maximum capacity of UHPC and HCSC specimens vs. time

Compared to the UHPC samples for Design 1, 2, and 3, the HCSC samples for Design 4 showed superior performance at an early age with an average pull-out capacity of about 40 kips (6 hrs).

At 12 hrs, the UHPC connection showed minimal capacity; however, the HCSC joint showed a capacity of more than 42 kips. At 24 hrs, the capacities of the HCSC (Design 4) and UHPC (Design 1) joints were similar, between 40 and 50 kips. Designs 2 and 3 showed comparative capacities to Design 4 after 1.5 days.

The research team observed that the samples located at the outermost edges of each concrete slab (exterior samples marked with 1 in Figure 36) showed a lower than anticipated capacity when compared with the interior samples (marked with 2 in Figure 36).
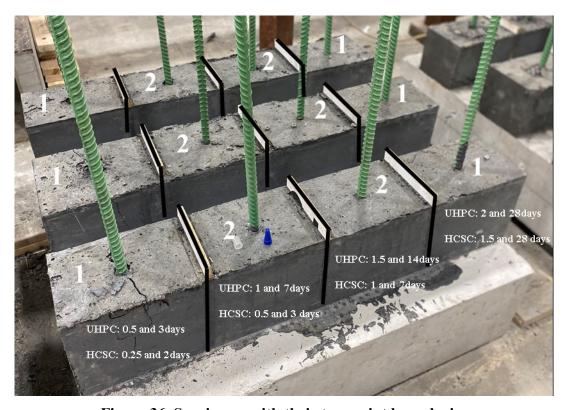

Figure 36. Specimens with their two-point boundaries

While the UHPC and HCSC materials were discontinuous between all samples, the interior samples were separated by 1/2 in. thick plywood. As the samples were tested, the failure mode typically involved a vertical split in the short direction of the specimen. Subsequently, the specimen pushed horizontally toward the adjacent specimen as the failure progressed. The plywood layer provided resistance to the horizontal movement given it was backed by the adjacent specimen. Specimens along the outer edge of the base slab only experienced resistance on one side.

To investigate how the specimen design and construction configurations affected the test results, the data were separated by one- and two-sided boundaries. Boundaries are represented by the black lines shown in Figure 36. The specimens marked with 1 have one-sided restraint, while those marked with 2 have two-sided restraint. UHPC samples for Designs 1, 2, and 3 that were tested at the ages of 0.5, 2, 3, and 28 days were considered as one-sided bounded specimens.

HCSC samples (Design 4) tested at the ages of 0.25, 1.5, 2, and 28 days were considered as one-sided bounded specimens.

The data in each group were used to establish the prediction curves. For example, with Design 1 specimens, the data from days 0.5, 2, 3, and 28 days (circles in Figure 37) were used to establish a prediction curve (dotted line) for the one-sided restraint situation.
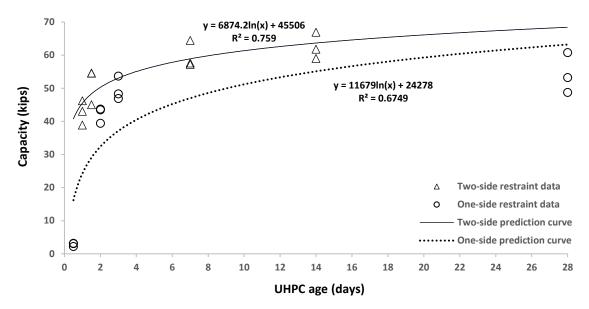

Figure 37. Restraint effects on Design 1

The data from days 1, 1.5, 7, and 14 days (triangles in Figure 37) were used to establish a prediction curve (solid line) for the two-sided restraint situation.

Figure 38, Figure 39, and Figure 40 show the restraint effects for Design 2, 3, and 4, respectively.
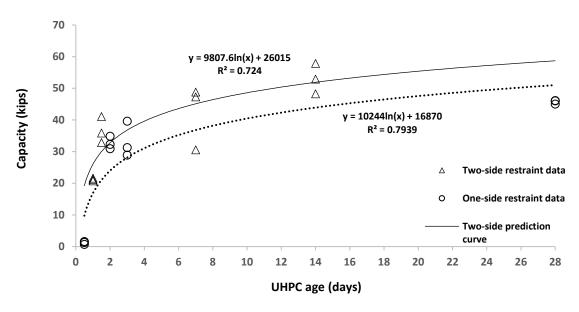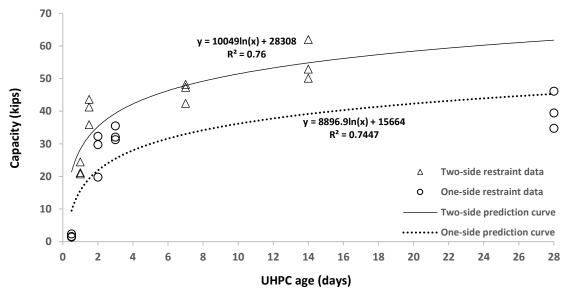
Figure 38. Restraint effects on Design 2

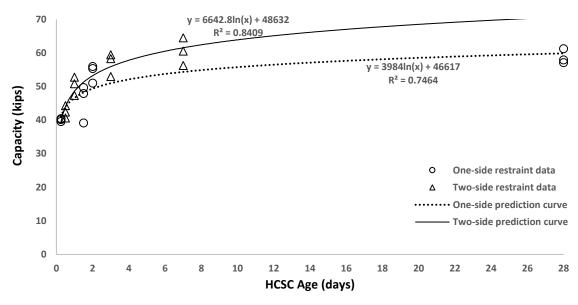**Figure 39. Restraint effects on Design 3**

Figure 40. Restraint effects on Design 4

In general, the two-sided restraint prediction curve gave a higher estimation of the capacities than the one-sided restraint situations. This matches the intuition that more lateral restraint provides resistance to crack development and leads to higher ultimate capacities.

For the UHPC connections (Design 1, 2, and 3), the difference in the capacity predictions between one-sided and two-sided restraints were about 10 to 20 kips. For the HCSC connections (Design 4), this difference was less than 10 kips.

Figure 42 and Figure 41 were plotted for one-sided and two-sided restraints, respectively. For both one-sided and two-sided restraint situations, the capacities for Design 4 were always higher than the other designs, especially at the early age of the material.

Figure 41. One-sided restraint effect for all designs

Design1 y = 11679ln(x) + 24278
R^2 = 0.6749

Design2 y = 10244ln(x) + 16870
R^2 = 0.7939

Design3 y = 8896.9ln(x) + 15664
R^2 = 0.7447

Design4 y = 6642.8ln(x) + 48632
R^2 = 0.7464

Figure 42. Two-sided restraint effect for all designs

Design1 y = 6874.2ln(x) + 45506
R^2 = 0.759

Design2 y = 9807.6ln(x) + 26015
R^2 = 0.724

Design3 y = 10049ln(x) + 28308
R^2 = 0.76

Design4 y = 6642.8ln(x) + 48632
R^2 = 0.8409

CHAPTER 6. SUMMARY, CONCLUSIONS, AND RECOMMENDATIONS

ABC offers several advantages to bridge construction projects including reduced impact to the traveling public and increased safety to onsite laborers. One form of ABC, SIBC is completed by constructing the bridge superstructure adjacent to the final alignment on temporary works, typically adjacent to the existing bridge being replaced. Upon completion, the superstructure is slid onto the permanent substructure. Once the slide is complete, closure joints between the bridge super- and sub-structure are cast to establish continuity. The time to complete the joint and the time-dependent cure of the fill materials establish when the bridge can be opened to traffic or construction loading.

The primary goal of this research was to investigate the performance of varying closure joint configurations reinforced with noncontact lap-spliced rebar and filled with UHPC, with a specific focus on determining when a noncontact lap splice has sufficient strength to either open a bridge or expose it to additional construction loading. A secondary goal of assessing an alternative material (HCSC) to UHPC to provide sufficient early-age capacity was also pursued.

To complete the research goals, a literature review was first conducted to collect and summarize the published information related to the performance of UHPC or HCSC closure joints reinforced with noncontact lap-spliced rebar. This was followed by laboratory work performed on 96 samples in four noncontact lap-splice connection designs with different rebar development lengths and joint filling materials. A time-dependent pull-out test was performed on each design with a focus on the performance of the material at early age. Each sample was loaded with a pull-out force until failure. The ultimate capacity of each sample was captured and analyzed. The key findings from this research were as follows:

- The UHPC material strength at an age of 12 hrs was insufficient to fully develop the reinforcement bars. At that time, the pull-out force for all three UHPC lap-splice designs (Design 1, Design 2, and Design 3) was less than 10% of the ultimate capacity at full strength. When the UHPC reached one day in age, Design 1 had a greater capacity than Design 2 or 3, and the rebar stress at failure for Design 1 exceeded the bar yield strength of 60 ksi. At 1.5 days, all UHPC connection designs reached the bar yield strength before failure.

- The compressive strength of the HCSC quickly increased to near full strength within the first 12 hrs. In fact, the pull-out force (40 kips) required to fail the HCSC connection (Design 4) exceeded the force at which the reinforcement bar yields (36 kips) at 6 hrs.

- The HCSC samples showed better performance with respect to the ultimate pull-out capacity than the UHPC samples during the earliest stages of material cure (before 1.5 days) when comparing the UHPC samples (Design 1, Design 2, and Design 3) to the HCSC samples (Design 4). HCSC gains strength quicker than the UHPC and could provide a solution for joint fill material if a very accelerated timeline is required (e.g., open bridge to traffic or construction loading in less than 24 hrs).

- Considering the cost of both materials, HCSC presents a viable alternative material to UHPC (similar minimum durability and strength properties exist) for short lap construction joints with SIBC and contributes to making SIBC cost competitive to staged construction.

- The lab test results showed that the confinement condition adjacent to the lap-spliced connection could affect the ultimate capacity. That is, when restraint to splitting failure mode due to continuous joint material adjacent to the point of interest exists, the ultimate capacity trends higher than the alternative. Hence, prediction equations with respect to one- and two-sided restraint situations were established for the estimation of the time-dependent ultimate capacities for each design.

With respect to the time-dependent performance of the noncontact lap-spliced connections evaluated as part of this research, the following recommendations are offered.

- **When using the development of bar yield strength as the minimum threshold for connection capacity, the connection can be considered for traffic or construction loading 24 hrs after the lap-spliced connection is placed if Design 1 is used, 36 hrs after construction when Designs 2 and 3 are used, and 6 hrs after construction when Design 4 is used.** The depth of connection, total lap length, bar configuration (straight/headed), and cementitious material varied between designs. Note that the capacities in this report are presented without factors of safety, the magnitude of which are left to be decided by the engineer.

- **Earlier age load application can be entertained when two-sided restraint is taken into consideration (as shown in the previous Figure 42)**. Based on the experimental results, pull-out capacities are affected by the presence of continuous joint material (UHPC or HCSC) and reinforcement adjacent to the bar being evaluated. The capacity requirement for the connection between the bridge super- and sub-structures will be uniquely calculated for each bridge structure. The researchers recommend that the prediction equations in the previous Figure 41 and Figure 42 be used to assess when the required capacity is met.

- **For the greatest capacity using UHPC, the researchers recommend Design 1 over Designs 2 and 3.** The ultimate capacities for the Design 1 samples tested at each prescribed point in time were always higher than those for Designs 2 and 3. Design 1 does require greater quantities of UHPC, which is likely to increase placement time and material costs.

- **For connections requiring very high early strength, the researchers recommend HCSC over UHPC.** The researchers further recommend working closely with the material supplier, particularly given the HCSC as mixed for this study had low flowability, which could impact complete fill of a gravity-fed closure pour. Discussion and effort to increase the flowability of the material is advised based on the research team's understanding that HCSC can be made more flowable without affecting the strength and durability attributes of the material.

- **When reduction of the total height of the closure pour connection is necessary, the researchers recommend that headed bars be considered for use given they offer capacities similar to straight rebar in connections of greater height.** Both Designs 2 and 3 were designed based on FHWA guidance (Graybeal 2014), and the results showed similar ultimate capacities for each design at each point in time during test completion.

REFERENCES

Alyousef, R., T. Topper, and A. Al-Mayah. 2018. Crack Growth Modeling of Tension Lap-Spliced Reinforced Concrete Beams Strengthened with Fibre Reinforced Polymer Wrapping under Fatigue Loading. *Construction and Building Materials*, Vol. 166, pp. 345–355.

Farzad, M., M., Shafieifar, and A. Azizinamini. 2019. Retrofitting of Bridge Columns Using UHPC. *Journal of Bridge Engineering*, Vol. 24, No. 12.

Fehling, E., P. Lorenz, and T. Leutbecher. 2012. Experimental Investigations on Anchorage of Rebars in UHPC. *Proceedings of the 2012 3rd International Symposium on UHPC and Nanotechnology for High Performance Construction Materials (HiPerMat)*, March 7–9, Kassel, Germany, pp. 533–540.

Grant, J. P. 2015. *Non-Contact Lap Splices in Dissimilar Concretes*. Master's thesis. Virginia Polytechnic Institute and State University, Blacksburg, VA

Graybeal, B. A. 2006. *Material Property Characterization of Ultra-High Performance Concrete*. FHWA-HRT-06-103. Turner-Fairbank Highway Research Center, McLean, VA.

Graybeal, B. A. 2010. *Field-Cast UHPC Connections for Modular Bridge Deck Elements*. Tech Brief FHWA-HRT-11-022. Federal Highway Administration, Turner-Fairbank Highway Research Center, McLean, VA.

Graybeal, B. 2014. *Design and Construction of Field-Cast UHPC Connections*. Tech Note FHWA-HRT-14-084/HRDI-40/10-14 (750) E. Federal Highway Administration, Turner-Fairbank Highway Research Center, McLean, VA.

Graybeal, B. A. and J. L. Hartmann. 2003. Strength and Durability of Ultra-High Performance Concrete. *Proceedings of the 2003 Precast Concrete Institute (PCI) National Bridge Conference*, October 19–22, Orlando, FL.

Graybeal, B. A. and J. Yuan. 2014. *Bond Behavior of Reinforcing Steel in Ultra-High Performance Concrete*. Tech Brief FHWA-HRT-14-089/HRDI-40/11-14 (300) E. Federal Highway Administration, Turner-Fairbank Highway Research Center, McLean, VA.

Haber, Z. B. and B. A. Graybeal. 2018. Lap-Spliced Rebar Connections with UHPC Closures. *Journal of Bridge Engineering*, Vol. 23, No. 6, Article 04018028.

Haber, Z. B., I. De la Varga, B. A. Graybeal, B. Nakashoji, and R. El-Helou. 2018. *Properties and Behavior of UHPC-Class Materials*. FHWA-HRT-18-036. Federal Highway Administration, Turner-Fairbank Highway Research Center, McLean, VA.

Hamad, B. S. and M. Y. Mansour. 1996. Bond Strength of Noncontact Tension Lap Splices. *Structural Journal*, Vol. 93, No. 3, pp. 316–326.

Harajli, M. H. 2009. Bond Stress–Slip Model for Steel Bars in Unconfined or Steel, FRC, or FRP Confined Concrete Under Cyclic Loading. *Journal of Structural Engineering*, Vol. 135, No. 5, pp. 509–518.

Hassan, T. K., G. W. Lucier, and S. H. Rizkalla. 2012. Splice Strength of Large Diameter, High Strength Steel Reinforcing Bars. *Construction and Building Materials*, Vol. 26, No. 1, pp. 216–225.

Hung, C.-C., S. El-Tawil, and S.-H. Chao. 2021. A Review of Developments and Challenges for UHPC in Structural Engineering: Behavior, Analysis, and Design. *Journal of Structural Engineering*, Vol. 147, No. 9, Article 03121001.

Karabinis, A. I. 2002. Reinforced Concrete Beam-Column Joints with Lap Splices under Cyclic Loading. *Structural Engineering and Mechanics*, Vol. 14, No. 6, pp. 649–660.

Kwik Bond Polymers, LLC. n.d. *Product Overview Sheet: Hybrid Composite Synthetic Concrete (HCSC).* https://issuu.com/kwikbondpolymers/docs/kbp-hcsc-overview-sheet?mode=window.

Liu, Z., K. S. Freeseman, J. M. Dahlberg, B. M. Phares, and M. LaViolette. 2021. *Lateral Slide of Multi-Span Bridges: Investigation of Connections and Other Details–Phase I.* Bridge Engineering Center, Iowa State University, Ames, IA.

Liu, Z., A. A. Semendary, and B. M. Phares. 2022. Numerical Investigation on Early Age Performance of Ultra-High-Performance Concrete Shear Keys Between an Adjacent Prestressed Concrete Box Beams. *Advances in Structural Engineering*, Vol. 25, No. 3, pp. 511–521.

Magureanu, C., I. Sosa, C. Negrutiu, and B. Heghes. 2012. Mechanical Properties and Durability of Ultra-High-Performance Concrete. *Materials Journal*, Vol. 109, No. 2, pp. 177–183.

McLean, D. I. and C. L. Smith. 1997. *Noncontact Lap Splices in Bridge Column-Shaft Connections*. Washington State Transportation Center, Washington State University, Pullman, WA.

Mousa, M. I. 2015. Flexural Behaviour and Ductility of High Strength Concrete (HSC) Beams with Tension Lap Splice. *Alexandria Engineering Journal*, Vol. 54, No. 3, pp. 551–563.

Najafgholipour, M. A., S. M. Dehghan, M. Khani, and A. Heidari. 2018. The Performance of Lap Splices in RC Beams under Inelastic Reversed Cyclic Loading. *Structures*, Vol. 15, pp. 279–291.

NYSDOT. 1997. *Test Mehod: 701-07 Anchoring Materials - Chemically Curing*. NY 701-14 E. New York State Department of Transportation, Materials Bureau, Albany, NY.

Perry, V. H. and P. Seibert. 2012. Field Cast UHPC Connections for Precast Bridge Elements and Systems. *Proceedings of the 2012 3rd International Symposium on UHPC and Nanotechnology for High Performance Construction Materials (HiPerMat)*, March 7–9, Kassel, Germany, pp. 669–678.

Ronanki, V. S., D. B. Valentim, and S. Aaleti. 2016. *Development Length of Reinforcing Bars in UHPC: An Experimental and Analytical Investigation*. First International Interactive Symposium on Ultra-High Performance Concrete – 2016, July 18–20, Des Moines, IA.

Sanchez, D. S. and L. R. Feldman. 2015. Effects of Transverse Bar Spacing on Bond of Spliced Reinforcing Bars in Fully Grouted Concrete Block Masonry. *Journal of Structural Engineering*, Vol. 41, No. 2.

Schuller, M. P., M. I. Hammons, and R. H. Atkinson. 1993. Interim Report on a Study to Determine Lap Splice Requirements for Reinforced Masonry. STP19607S. *Masonry: Design and Construction, Problems and Repair*. ASTM Committees, December 1992, Miami, FL.

Semendary, A. A., K. K. Walsh, and E. P. Steinberg. 2017. Early-Age Behavior of an Adjacent Prestressed Concrete Box-Beam Bridge Containing UHPC Shear Keys with Transverse Dowels. *Journal of Bridge Engineering*, Vol. 22, No. 5, Article 04017007.

Shafieifar, M., M. Farzad, and A. Azizinamini. 2018. New Connection Detail to Connect Precast Column to Cap Beam using Ultra-High-Performance Concrete in Accelerated Bridge Construction Applications. *Transportation Research Record: Journal of the Transportation Board*, Vol. 2672, No. 41, pp. 207–220.

Tarquini, D., J. P. de Almeida, and K. Beyer. 2019. Experimental Investigation on the Deformation Capacity of Lap Splices under Cyclic Loading. *Bulletin of Earthquake Engineering*, Vol. 17, No. 12, pp. 6645–6670.

Toledo, W. K., L. Davila, A. J. Al-Basha, C. M. Newtson, and B. D. Weldon. 2020. Assessment of Ultra-High Performance Concrete Overlays on Concrete Bridge Decks. *Tran-SET 2020*, September 1–2, Albuquerque, NM.

Varbel, J. M., E. Y. Flores, W. K. Toledo, C. M. Newtson, and B. D. Weldon. 2020. *Structural Testing of Ultra-High Performance Concrete Shear Keys in Concrete Bridge Superstructures*. Tran-SET 2020, September 1–2, Albuquerque, NM.

Wagner, E. I. and P. D. Krauss. 2020. *Bond Behavior of Reinforcing Steel in Kwik Bond HCSC Material*. Final Report for Kwik Bond Polymers WJE No. 2006.4138.8. Wiss, Janney, Elstner Associates, Inc., Northbrook, IL.

Zhao, S., E. Van Dam, D. Lange, and W. Sun. 2017. Abrasion Resistance and Nanoscratch Behavior of an Ultra-High Performance Concrete. *Journal of Materials in Civil Engineering*, Vol. 29, No. 2, Article 04016212.

THE INSTITUTE FOR TRANSPORTATION IS THE FOCAL POINT FOR TRANSPORTATION AT IOWA STATE UNIVERSITY.

InTrans centers and programs perform transportation research and provide technology transfer services for government agencies and private companies;

InTrans contributes to Iowa State University and the College of Engineering's educational programs for transportation students and provides K–12 outreach; and

InTrans conducts local, regional, and national transportation services and continuing education programs.

Visit **InTrans.iastate.edu** for color pdfs of this and other research reports.